Bulletin of Mathematical Biology (1998) **60**, 329–353

In vitro DNA-based Predator–Prey System with Oscillatory Kinetics

J. ACKERMANN, B. WLOTZKA AND J. S. MCCASKILL
Institut für Molekulare Biotechnologie (IMB),
Beutenbergstraße 11,
D–07745 Jena, Germany
E-mail: jack@imb-jena.de

A coupled system of two isothermal *in vitro* DNA/RNA amplification reactions using different primers is modeled kinetically with realistic rate parameters and shown to exhibit oscillatory behavior in a flow reactor. One of the two isothermal amplification reactions acts as a predator of the other, the prey. The mechanism of the oscillatory behavior is analyzed in terms of a hierarchy of kinetic models. The work provides an insight into the choice of parameters for experiments. The latter are important in providing detailed insight into the complex processes of ecological interactions and their evolution.

1. INTRODUCTION

Our knowledge of the evolutionary phenomena has increased markedly in precision since the first *in vitro* evolution experiments (Spiegelmann, 1971). The use of well-characterized and isolated enzymes demonstrates the quantitative implications of a genotype–phenotype relationship mediated by well-defined kinetic and structural principles (e.g. RNA folding) (Biebricher *et al*., 1983, 1984, 1985). New principles of evolution relevant to the search for early biological function and modern virus evolution have been uncovered (Eigen, 1989). Although early work was quick to highlight the importance of the big question of the origin of cooperation between molecules (Eigen, 1971), the above-mentioned work with the Qß enzyme has not allowed the level of control required for a programmed coupling of different amplification cycles *in vitro*.

Furthermore, it has become very clear that the stabilization of cooperative functions of biomolecules depends not only on the mode of functional coupling of amplification, as in the work on hypercycles (Eigen and Schuster, 1977), but also crucially on spatial properties such as compartmentation (Bray, 1980). This has prompted some groups to shift the search to autonomous systems of coupled oligonucleotide amplification and division of micelles (Luisi *et al*., 1994). In recent work, however, it has been possible to show that spatial stabilization of cooperation can be attained without the need for artificial compartments, by means of pattern forming reaction diffusion processes (Boerlijst and Hogeweg, 1991;

0092-8240/98/020329 + 25 $25.00/0 bu970001

Böddeker and McCaskill, 1998). Since oscillatory kinetics in a homogeneous setting are strongly correlated with the ability of a reaction diffusion system to show complex pattern formation (Murray, 1982), it is important to investigate the conditions under which coupled oligonucleotide amplification systems can show oscillatory behavior.

Hypercyclic coupling of self-replicating species in a ring with more than four members has been shown to give rise to limit cycle oscillations (Eigen and Schuster, 1977; Eigen and Schuster, 1978a; Eigen and Schuster, 1978b; Hofbauer and Sigmund, 1988). Such complex coupling is difficult to realize experimentally, however, due to the large number of specific interactions required. Ecologically, the earliest recognized, and perhaps the simplest, form of coupling investigated was that by Lotka (1910, 1920) and Volterra (1926, 1931) (Lotka was the first to write down the equations for a hypothetical chemical system, followed by the biologically inspired Volterra). This predator–prey coupling is not cooperative, but the evolution of non-virulent forms of viruses does show us that such systems can also give some insight into cooperation. In a separate investigation, the authors have planned an extension to truly cooperative experimentally feasible coupling schemes.

Self-sustained sequence replication (known as 3SR) (Guatelli *et al*., 1990) is an isothermal amplification scheme (in contrast to PCR) for the coupled amplification of both DNA and RNA oligomers. The cyclic coupling scheme is shown in Fig. 1. The 3SR-reaction is performed by the concerted action of an RNA-polymerase (T) and a reverse transcriptase (RT). These two enzymes implement transcription, whereby single-stranded RNA oligomers are transcribed from the double-stranded DNA template starting after a specific promoter sequence on the DNA, and reverse transcription in which double-stranded DNA is synthesized from a single-stranded RNA template in a multistep process. During multiple cycles of transcription and reverse transcription RNA and DNA are amplified jointly.

In order to establish a basis for the investigation of coupled 3SR reactions, in Section 2 we summarize the known features of 3SR kinetics and propose a simplified kinetic model. In Section 3, we present the proposed mechanism for coupling 3SR amplification schemes as predator and prey and outline a kinetic model for describing the coupled system. In order to gain a better understanding of what features of the mechanism and parameters give rise to oscillatory behavior, we compare these results with reduced kinetic schemes, which allows a direct comparison with conventional predator–prey results. In Section 4 we present our conclusions on the viable range of parameters for limit cycle predator–prey kinetics of coupled 3SR reactions in flow reactors and provide a preliminary discussion of the evolutionary features of such model systems.

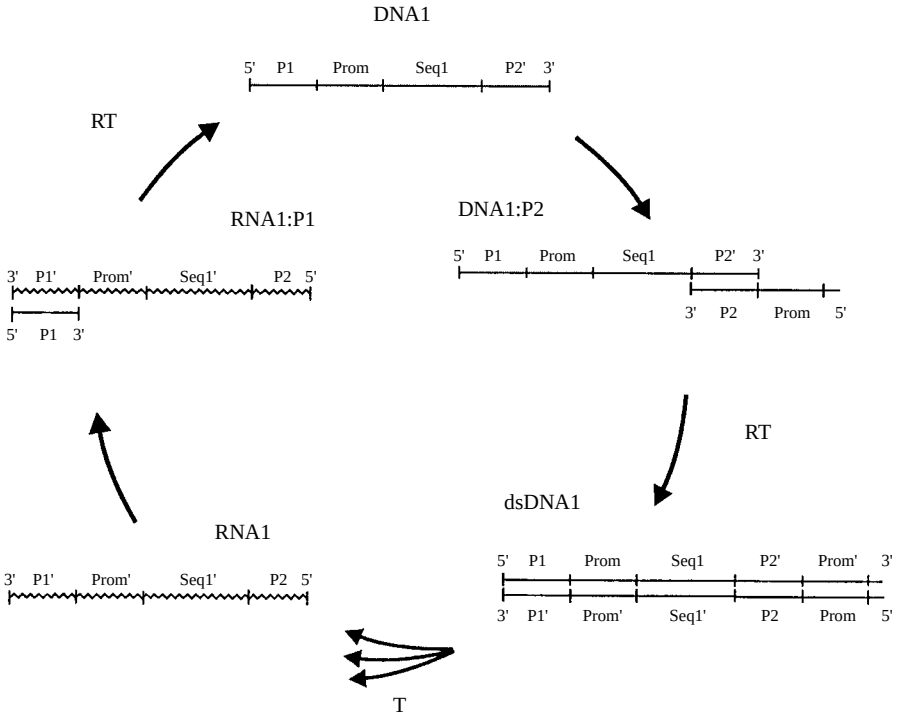

Figure 1. Reaction scheme of the 3SR-amplification. The 3SR reaction is performed by the concerted action of a RNA-polymerase (T) and a reverse transcriptase (RT). During multiple cycles of transcription and reverse transcription, RNA and DNA can be amplified at the same time. The reaction is started from a synthetic, single-stranded DNA template. Annealing of a DNA-primer P2 containing the promoter sequence for the RNA-polymerase and subsequent generation of a fully double-stranded species by the action of RT produces a substrate for *in vitro*-transcription by RNA-pol. Multiple copies of antisense-RNA are synthesized. Another DNA-primer, P1, initiates reverse transcription. The cycle is closed by simultaneous degradation of the RNA-strand by RNAse activity of RT resulting in new single-stranded DNA. Straight lines refer to DNA and waved lines refer to RNA. The abbreviations for the modules building the whole sequence are: P1, P2 for primer sites, the RNA-polymerase promoter PROM and Seq1 for a fixed sequence without any special function. Complementary sequences of the modules are indicated by a prime. Numbers at the beginning and end of each sequence refer to the direction of the sequence. Additional abbreviations are T for RNA-polymerase and RT for reverse transcriptase.

2. KINETIC MODEL

Each of the steps of the 3SR reaction mentioned above is a complicated sequence- dependent biochemical process. Its complexity is beyond the scope of an exact theoretical description. For an understanding of some of the successively detailed levels of modeling required even for a simpler replication reaction, in particular the monomer dependence, see Biebricher *et al.* (1983, 1984, 1985). We model the 3SR scheme in terms of the simplified chemical reactions:

$$\begin{array}{lcll}
\mathrm{DNA} & + \mathrm{P2} & \xrightarrow{k_1} & \mathrm{DNA:P2} \\
\mathrm{DNA:P2} & + \mathrm{RT} & \xrightarrow{k_2} & \mathrm{DNA:P2:RT} \\
\mathrm{DNA:P2:RT} & & \xrightarrow{k_3} & \mathrm{ds\,DNA} + \mathrm{RT} \\
\mathrm{ds\,DNA} & + \mathrm{T} & \xrightarrow{k_4} & \mathrm{ds\,DNA:T} \\
\mathrm{ds\,DNA:T} & & \xrightarrow{k_5} & \mathrm{RNA} + \mathrm{T} + \mathrm{ds\,DNA} \\
\mathrm{RNA} & + \mathrm{P1} & \xrightarrow{k_6} & \mathrm{RNA:P1} \\
\mathrm{RNA:P1} & + \mathrm{RT} & \xrightarrow{k_7} & \mathrm{RNA:P1:RT} \\
\mathrm{RNA:P1:RT} & & \xrightarrow{k_8} & \mathrm{DNA} + \mathrm{RT}\,.
\end{array} \tag{1}$$

In arriving at (1) the following assumptions have been made:

- The nucleotide concentrations needed for the DNA and RNA polymerizations processes are constant; as is the case for example with an excess of these nucleotides.
- The reactions where the enzymes RNA-polymerase and reverse transcriptase act simultaneously in one complex play a minor role for the kinetics. Thus, the RNA-polymerase and reverse transcriptase activities are assumed to act independently.
- The activities of reverse transcriptase and the RNAse can be described by a single reaction. Reverse transcriptase proceeds via a RNA–DNA heteroduplex, the RNA of which is digested by the nuclease activity of RT.
- Dead end side reactions as well as dissociation processes are neglected.
- The finite lifetime of the enzymes are neglected.

Some of these assumptions are—of course—not valid in all real-life 3SR experiments. The effect of dead end side reactions as well as dissociation reactions may be very important in certain cases, but we found them not to influence the main findings of this work. Other assumptions, such as the neglect of the finite enzyme lifetime or of the finite monomer concentration, are not satisfied for long reaction times under batch conditions, but are valid in a flow reactor where the monomer and enzymes are added continuously in the influx. In a flow reactor, the following terms must be added:

$$C \xrightarrow{\phi} \emptyset \qquad \text{for } C \in \mathcal{M}$$

$$\emptyset \xrightarrow{\phi\,[C]_{flux}} C \qquad \text{for } C \in \{\mathrm{P1}, \mathrm{P2}, \mathrm{RT}, \mathrm{T}\}$$

$\mathcal{M}$ is the set of all chemical species involved in the reaction scheme, the constant ϕ is the flow rate and $[C]_{\mathrm{flux}}$ is the concentration of a certain species in the influx. The case $\phi = 0$ reduces to a well-mixed reactor without any flux. Such a choice for the flux reactions is motivated by the simplicity of its experimental realization. All species (enzymes, primers, RNA, DNA, complexes) are diluted by the outflow and if the reaction is not to die out, this effect must be compensated by the amplification reaction. Since the primers and enzymes (and the monomers) are not amplified, they must be added in the influx. An amplification reaction started by adding a low template concentration at the outset can work for arbitrary long time at high DNA/RNA concentration in this way. The DNA/RNA concentration in the out flux can be optimized by the flow rate and the experimental study of evolutionary effects in such a simple flow reactor should be worthwhile. In an economical reactor, an immobilization of the enzymes may be advisable, but due to the finite lifetime of the enzymes this reduces the long time stability of the effects described later.

In the following, we first wish to discuss the reaction system (1) for the case where the flow rate is zero. Later in this section we return to the case of non-zero flux. The 3SR reaction is usually started with a low template (RNA or DNA) concentration:

$$\max([\mathrm{RNA}]_0,\ [\mathrm{DNA}]_0) \quad \ll \quad \min([\mathrm{P1}]_0,\ [\mathrm{P2}]_0,\ [\mathrm{RT}]_0,\ [\mathrm{T}]_0). \tag{2}$$

Hereafter we use the convention to denote chemical species by capital letters, whereas [ ] or the corresponding lower case letter denotes the concentration of the species. The index 0 indicates the concentration at $t = 0$. While the concentration of RNA and DNA are low, the primer and enzyme concentrations are assumed to be constant in the initial phase. Thus, the above reaction system is reduced to the linearized system:

$$\begin{aligned}
\mathrm{DNA} &\xrightarrow{k_1[\mathrm{P2}]_0} \mathrm{DNA : P2}\\
\mathrm{DNA : P2} &\xrightarrow{k_2[\mathrm{RT}]_0} \mathrm{DNA : P2 : RT}\\
\mathrm{DNA : P2 : RT} &\xrightarrow{k_3} \mathrm{ds\,DNA}\\
\mathrm{ds\,DNA} &\xrightarrow{k_4[\mathrm{T}]_0} \mathrm{ds\,DNA : T}\\
\mathrm{ds\,DNA : T} &\xrightarrow{k_5} \mathrm{RNA} + \mathrm{ds\,DNA}\\
\mathrm{RNA} &\xrightarrow{k_6[\mathrm{P1}]_0} \mathrm{RNA : P1}\\
\mathrm{RNA : P1} &\xrightarrow{k_7[\mathrm{RT}]_0} \mathrm{RNA : P1 : RT}\\
\mathrm{RNA : P1 : RT} &\xrightarrow{k_8} \mathrm{DNA}\,.
\end{aligned}$$

The system of ordinary differential equations for the vector of concentrations $\vec{C}$ (the species are ordered as they occur in the above reaction system, $C_1 = [\mathrm{DNA}]$, $C_2 = [\mathrm{DNA} : \mathrm{P2}]$, ...) takes the form:

$$\frac{d\vec{C}}{dt} = \mathbf{A}\vec{C} \tag{3}$$

$$\begin{aligned} \tilde{k_1} &:= k_1[\mathrm{P2}]_0, \qquad \tilde{k_2} := k_2[\mathrm{RT}]_0, \\ \tilde{k_4} &:= k_4[\mathrm{T}]_0, \qquad \tilde{k_6} := k_6[\mathrm{P1}_0, \qquad \tilde{k_7} := k_7[\mathrm{RT}]_0 \end{aligned} \tag{4}$$

with

$$\mathbf{A} = \begin{pmatrix} -\tilde{k_1} & 0 & 0 & 0 & 0 & 0 & 0 & k_8 \\ \tilde{k_1} & -\tilde{k_2} & 0 & 0 & 0 & 0 & 0 & 0 \\ 0 & \tilde{k_2} & -k_3 & 0 & 0 & 0 & 0 & 0 \\ 0 & 0 & k_3 & -\tilde{k_4} & \mathbf{k_5} & 0 & 0 & 0 \\ 0 & 0 & 0 & \tilde{k_4} & -k_5 & 0 & 0 & 0 \\ 0 & 0 & 0 & 0 & k_5 & -\tilde{k_6} & 0 & 0 \\ 0 & 0 & 0 & 0 & 0 & \tilde{k_6} & -\tilde{k_7} & 0 \\ 0 & 0 & 0 & 0 & 0 & 0 & \tilde{k_7} & -k_8 \end{pmatrix}. \tag{5}$$

Except for the item in bold face, the matrix represents a simple cycle of transformations. The regeneration of ds DNA following transcription (boldface entry) is responsible for the net amplification of the cycle.

In the following we will assume the primer and enzyme association rates to be fast compared with the activities of the enzymes:

$$\min(\tilde{k_1}, \tilde{k_2}, \tilde{k_4}, \tilde{k_6}, \tilde{k_7}) \quad \gg \quad \max(k_3, k_5, k_8). \tag{6}$$

This may not be satisfied for every 3SR replication cycle. The binding of the RNA-polymerase, for example, includes a promoter recognition step, which may be slow depending on the promoter sequence. In such a case, the promoter recognition step and the transcription step of the RNA-polymerase can be combined to create one slow enzyme reaction; i.e. to k_5.

Assumption (6) introduces two timescales: one for the fast bindings and the other for the slow activities of the enzymes. For very short reaction times, $t \ll 1/\max(k_3, k_5, k_8)$, we can neglect the enzyme activities. Note that the sum of the concentrations of the three species DNA, DNA : P2, DNA : P2 : RT is constant on this time scale. This illustrates a more general feature of the reaction: on the timescale of the enzyme activities we can assume the fast reactions to be in a steady state. This motivates the introduction of the three lumped concentrations

$$[\mathrm{DNA}'] = [\mathrm{DNA}] + [\mathrm{DNA} : \mathrm{P2}] + [\mathrm{DNA} : \mathrm{P2} : \mathrm{RT}]$$

$$[\mathrm{ds\,DNA}'] = [\mathrm{ds\,DNA}] + [\mathrm{ds\,DNA} : \mathrm{T}]$$

$$[\mathrm{RNA}'] = [\mathrm{RNA}] + [\mathrm{RNA} : \mathrm{P1}] + [\mathrm{RNA} : \mathrm{P1} : \mathrm{RT}],$$

which for (6) are approximately given by

$$[\mathrm{DNA}'] \approx [\mathrm{DNA} : \mathrm{P2} : \mathrm{RT}]$$

$$[\mathrm{ds\,DNA}'] \approx [\mathrm{ds\,DNA} : \mathrm{T}]$$

$$[\mathrm{RNA}'] \approx [\mathrm{RNA} : \mathrm{P1} : \mathrm{RT}].$$

In this case, the time dependency of the lumped concentrations is given by the simple system of ordinary differential equations (ODEs):

$$\frac{d\vec{C}}{dt} = \mathbf{A}\vec{C} \tag{7}$$

with

$$\mathbf{A} := \begin{pmatrix} -k_3 & 0 & k_8 \\ k_3 & 0 & 0 \\ 0 & k_5 & -k_8 \end{pmatrix} \tag{8}$$

and $\vec{C} := ([\mathrm{DNA}'],\ [\mathrm{ds\,DNA}'],\ [\mathrm{RNA}'])^{\mathrm{T}}$. ODE (7) corresponds to the reaction system

$$\begin{aligned} \mathrm{DNA}' &\xrightarrow{k_3} \mathrm{ds\,DNA}' \\ \mathrm{ds\,DNA}' &\xrightarrow{k_5} \mathrm{RNA}' + \mathrm{ds\,DNA}' \\ \mathrm{RNA}' &\xrightarrow{k_8} \mathrm{DNA}'. \end{aligned} \tag{9}$$

for three 'lumped species' DNA′, ds DNA′, and RNA′. Note that the linearization of the full system (1) is not necessary to arrive at the small ODE (7); but illustrates the chemical conditions for this simplification.

In the non-degenerate case, the solution of this ODE can be expressed in terms of the eigenvalues $(\lambda_i, i = 1, 2, 3)$ and the eigenvectors $(\vec{x}_i, i = 1, 2, 3)$ of the matrix **A**:

$$\vec{C} = \gamma_1 \vec{x}_1 e^{\lambda_1 t} + \gamma_2 \vec{x}_2 e^{\lambda_2 t} + \gamma_3 \vec{x}_3 e^{\lambda_3 t} \tag{10}$$

with constants $\gamma_i, i = 1, 2, 3$. The eigenvalues are given by the roots of the equation

$$\lambda^3 + \lambda^2(k_3 + k_8) + \lambda k_3 k_8 - k_3 k_5 k_8 = 0. \tag{11}$$

The analytical expressions for the eigenvalues and eigenvectors are straightforward but not especially illuminating. A general feature of the solution may be seen from the special case $k_3 = k_5 = k_8 = k$ which yields one dominant positive eigenvalue $\lambda_1 \approx 0.47k$ and a pair of complex conjugated eigenvalues $\lambda_{2,3} \approx (-1.2 \pm 0.79i)k$. In general, the real part of the complex eigenvalue pair is negative, the initial oscillatory behavior of the solution will die out rapidly

and is not the subject of this paper. For longer times the concentration will grow exponentially ($\sim \exp(\lambda_1 t)$). The solution of (9) takes the form

$$\begin{pmatrix} [\mathrm{DNA}'] \\ [\mathrm{ds\,DNA}'] \\ [\mathrm{RNA}'] \end{pmatrix} \sim \begin{pmatrix} 1 \\ K_1 \\ K_2 \end{pmatrix} \exp(\lambda_1 t) \tag{12}$$

where the constant ratios $K_1 = [\mathrm{ds\,DNA}']/[\mathrm{DNA}']$ and $K_2 = [\mathrm{RNA}']/[\mathrm{DNA}']$ are determined by the relative proportions $k_1 : k_2 : k_3$.

However, even for infinitely fast complex formation reactions, the part of the lumped species which exists as end product of these fast reactions is limited by the finite primer and enzyme concentrations. For example, the concentration of the complex DNA : P2 : RT cannot exceed the initial concentration of the primer P2 minus the part of this concentration already consumed to produce double-stranded DNA. These types of limitations lead to constraints of the form:

complex		limiting function	limited by
[DNA : P2 : RT]	$\leq$	$f_1 = [\mathrm{P2}]_0 - [\mathrm{ds\,DNA}']$	P2
[DNA : P2 : RT]	$\leq$	$f_2 = [\mathrm{RT}]_0 - [\mathrm{RNA : P1 : RT}]$	RT
[ds DNA : T]	$\leq$	$f_3 = [\mathrm{T}]_0$	T
[RNA : P1 : RT]	$\leq$	$f_4 = [\mathrm{RT}]_0 - [\mathrm{DNA}']$	RT
[RNA : P1 : RT]	$\leq$	$f_5 = [\mathrm{P1}]_0 + [\mathrm{DNA}]_0$ $-[\mathrm{DNA}'] - [\mathrm{ds\,DNA}']$	P1

(13)

When the concentration of these species reach their limiting values, they become constant or drop exponentially to zero, depending on whether the limitation is induced by the enzymes (f_2, f_3, f_4) or by the primer depletion (f_1, f_5). In which order these constraints influence the reaction plays a crucial role for the kinetic behavior of the 3SR reaction. Since these constraints can set in at four different time points, one for each of the primer concentrations and one for each of the enzyme concentrations, there exist $4!(= 24)$ different orders in which the above constraints may set in. Each case must be analyzed separately. Here we present the procedure for one case and leave the reader to apply the procedure to other cases of interest.

In Fig. 2 the concentration of the complexes DNA : P2 : RT, ds DNA : T and RNA : P1 : RT is plotted for $k_1 = k_2 = k_3 = k = 0.005$. In the initial phase, all concentrations grow exponentially and the concentrations of the complexes are identical with the concentrations of the corresponding lumped species. The saturation of the reverse transcriptase sets in at t_1, when f_2 (dotted line) crosses the concentration of DNA : P2 : RT. Now the concentrations of the complexes DNA : P2 : RT and RNA : P1 : RT become constant (here we neglect a possible small change in the RNA/DNA ratio). At t_2 the concentration of free primers P2 becomes zero and f_1 crosses the constant concentration of DNA : P2 : RT.

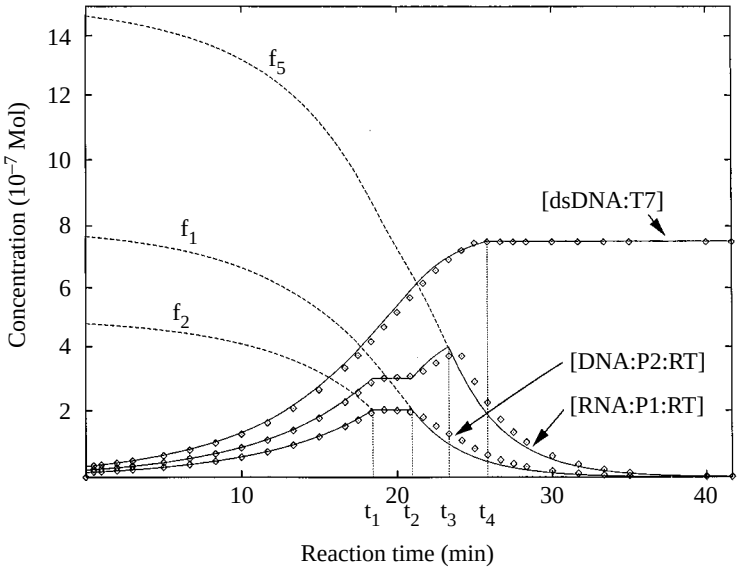

Figure 2. An example for different time phases of the 3SR reaction. Plotted are the analytical forms (solid lines) and numerical results (asterisks) for the concentrations of the complexes ds DNA : T, DNA : P2 : RT and RNA : P1 : RT. The exponential growth at the beginning is limited by the saturation of the reverse transcriptase enzymes. The time point for this limitation is t_1, where $f_2 = [\mathrm{RT}]_0 - [\mathrm{RNA} : \mathrm{P1} : \mathrm{RT}]$ (dotted line) crosses [DNA : P2 : RT]. Similar limitations occur at the time points t_2 (exhaustion of primer P_2), t_3 (exhaustion of primer P_1) and t_4 (saturation of RNA-polymerase), see text.

No more complexes DNA : P2 : RT can be built due to the lack of free primers P2 and the concentration of the DNA : P2 : RT complex drops exponentially to zero. The emerging free enzymes RT react instantaneously to the complex RNA : P1 : RT. Hence [RNA : P1 : RT] crosses f_5 at t_3 and the lack of the primer P1 for $t > t_3$ results in an exponential decreasing concentration of this complex. The concentration of the complex ds DNA : T can be computed directly from the concentration of the complex DNA : P2 : RT; exponential growth for $t < t_1$, linear growth for $t_1 < t < t_2$, which ascent drops continuously to zero for $t > t_2$; at t_4 [ds DNA : T] reaches the initial concentration of the RNA-polymerase. The analytical form of the concentrations can be derived easily in this piecewise fashion. The corresponding concentrations resulting from a numerical simulation of the full model are plotted in Fig. 2 as diamonds. There is a good agreement between the results of the simple approximation described above and the accurate numerical results; only near t_2 and t_3 does the continuous drop to zero of the primer concentration smoothen the peaks of the curves.

In general, the 3SR reaction shows a sequence of kinetic regimes, starting with an exponential growth and changing at certain titration endpoints to primer or enzyme limited kinetics. The order and duration of these regimes depend on the initial concentrations and the kinetic parameters. Within these regimes, the time

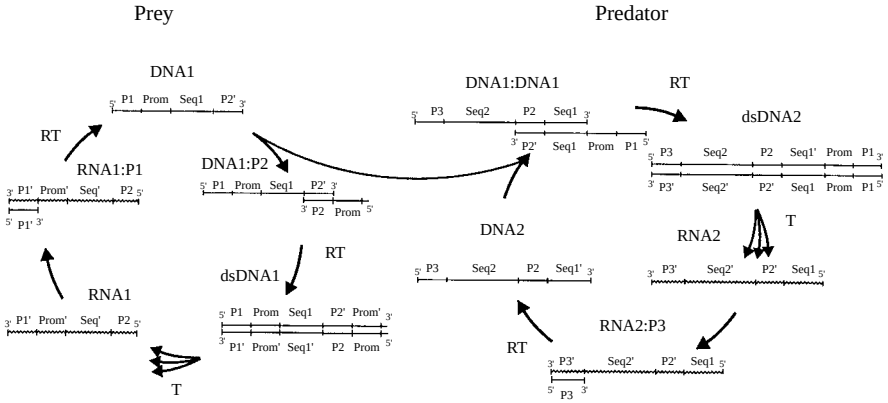

Figure 3. Reaction scheme of the predator–prey system. (Notations as used in Fig. 1.) The 3SR reaction on the left-hand side is described in detail in Fig. 1. The coupling of two amplification systems is designed according to a predator–prey model by using an intermediate of the first replication cycle (prey, left-hand side) as a primer for the second one (predator, right-hand side). The predator cycle is only provided with the primer for starting reverse transcription. The second primer is the single-stranded template DNA_1 of the prey cycle. The sequence of this template DNA_1 is designed so that predator template DNA_2 and prey template DNA_1 share complementary sequence elements at their 3′-ends. The promoter sequence of RNA-pol is located upstream of this complementary sequence element on DNA_1. After annealing of DNA_2 and DNA_1, RT can synthesize the double-stranded substrate for RNA-pol, which can start the *in vitro* transcription of antisense predator RNA.

dependence of the concentrations can be described quite well in an analytical form as described above. Experimentally the amplification of RNA and DNA products is usually monitored through the incorporation of radio-labeled primers. On-line monitoring is possible when measuring the increase in fluorescence intensity of intercalating agents. Examples can be found in the work of Gebinoga and Oehlenschläger (1996), who used this method to compare different 3SR-systems, or in the work of Ehricht *et al*. (1997), who used the intercalating dye ToPro-1 to study their cooperatively coupled 3SR system (CATCH) (Ehricht *et al*., 1997). Such experimental curves can be compared with the theoretical dynamics described above and these new insights into the reaction dynamic can be used to optimize the 3SR reaction.

In this context the following considerations are helpful. For given kinetic parameters, we can choose initial primer and enzyme concentrations so that the time points t_1, t_2, t_3 and t_4 become equal. This corresponds to an optimal use of primer and enzymes to enlarge the exponential growth phase. The conditions are

$$\frac{[\mathrm{P1}]_0 + [\mathrm{DNA}]_0 + [\mathrm{ds\,DNA}]_0}{K_1 + K_2 + 1} = \frac{[\mathrm{P2}]_0 + [\mathrm{ds\,DNA}]_0}{K_1 + 1} = \frac{[\mathrm{T}]_0}{K_1} = \frac{[\mathrm{RT}]_0}{K_2 + 1} \qquad (14)$$

with the constants K_1 and K_2 from (12).

Another goal is the optimization of the 3SR in the latter linear RNA growth phase. Independently of the order of limitation (13), the concentration of the

complexes DNA : P2 : RT and RNA : P1 : RT will drop essentially to zero for long reaction times, since only the RNA concentration grows linearly. The growth rate in this linear phase depends either on the concentration of the double-stranded DNA or on the concentration of the RNA-polymerase available. The concentration of the double-stranded DNA depends on the initial primer concentrations:

$$p_{\min} := \lim_{t\to\infty} ([\text{ds DNA}] + [\text{ds DNA} : \text{T}]) = \min([\text{P2}]_0, ([\text{P1}]_0 + [\text{DNA}]_0)). \quad (15)$$

The linear growth rate RNA is determined by the actual concentration of the ds DNA : T complex:

$$[\text{RNA}] = A + k_5\ [\text{ds DNA} : \text{T}]_{t\to\infty} t, \quad (16)$$

with an offset constant A. The asymptotic concentration of ds DNA:T is given by

$$[\text{ds DNA} : \text{T}]_{t\to\infty} = \frac{1}{2}\left(\frac{k_5}{k_4} + p_{\min} + [\text{T}]_0\right) - \sqrt{\frac{1}{4}\left(\frac{k_5}{k_4} + p_{\min} + [\text{T}]_0\right)^2 - p_{\min}[\text{T}]_0}. \quad (17)$$

The linear growth rate simplifies in the asymptotic cases

$$\begin{aligned} &[\text{RNA}] \approx A + k_4\ p_{\min}[\text{T}]_0 && \text{for} \quad k_5/k_4 \gg \max([\text{T}]_0, p_{\min}) \\ &[\text{RNA}] \approx A + k_5\ [\text{T}]_0 t && \text{for} \quad [\text{T}]_0 \gg \max(p_{\min}, k_5/k_4) \\ &[\text{RNA}] \approx A + k_5\ p_{\min} t && \text{for} \quad p_{\min} \gg \max([\text{T}]_0, k_5/k_4). \end{aligned} \quad (18)$$

Thus for small primer and enzyme concentrations (compared with k_5/k_4) the yield of the 3SR reaction can be optimized by increasing either the initial RNA-polymerase concentration or the initial primer concentrations. The primers P1 and P2 should be added in equal concentrations.

For large initial concentrations the situation changes. If RNA-polymerase is already given in unbalanced excess, an increase in this particular concentration will have no (positive) effect. In contrast, the same is true for the primer concentration; the initial concentrations of the primers and the RNA-polymerase should be of the same order $[\text{P1}]_0 \approx [\text{P2}]_0 \approx [\text{T}]_0$.

Let us now turn to the non-zero flux case. The main effect of the flux to a 3SR reaction can be illustrated by considering the simple kinetic model system

$$\text{RNA} + \text{P} \xrightarrow{k_1} \text{ds DNA} \xrightarrow{k_2} \text{ds DNA} + \text{RNA}, \quad (19)$$

which—like the full reaction system (1)—shows an initial exponential growth phase and a long-time linear growth phase. The flux is modeled by the reactions

$$\begin{aligned} \text{ds DNA} &\xrightarrow{\phi} \emptyset \\ \text{RNA} &\xrightarrow{\phi} \emptyset \\ \text{P} &\xrightarrow{\phi} \emptyset \\ \emptyset &\xrightarrow{\phi\,[\text{P}]_0} \text{P}\,. \end{aligned}$$

Switching on the flow term, we obtain a finite non-trivial steady state:

$$[\text{P}] = \frac{\phi^2}{(k_2 - \phi)k_1}, \qquad [\text{ds DNA}] = [\text{P}]_0 - \frac{\phi^2}{(k_2 - \phi)k_1}, \tag{20}$$

$$[\text{RNA}] = \frac{k_2 - \phi}{\phi}[\text{P}]_0 - \frac{\phi}{k_1}. \tag{21}$$

The non-trivial steady state turns into the trivial one:

$$[\text{P}] = [\text{P}]_0, \qquad [\text{ds DNA}] = 0, \qquad [\text{RNA}] = 0 \tag{22}$$

for flow rates greater than a critical flow rate

$$\phi_c = \frac{k_1[\text{P}]_0}{2}\left(\sqrt{1 + \frac{4k_2}{[\text{P}]_0 k_1}} - 1\right), \tag{23}$$

which for $[\text{P}_0] \gg 4k_2/k_1$ is simply given by the RNA transcription rate

$$\phi_c = k_2. \tag{24}$$

Analysis of the full kinetic model (1) confirms this critical behavior. Below this critical flow rate, the flow rate may be chosen to place the reaction in one of kinetic regimes determined by the constraints (13). For values close to the critical flow rate the reaction approaches the exponential growth phase, where none of these limits has been reached. The critical flow rate is an important indicator for the range of flow rates, where complex patterns can be expected in one- and two-dimensional flow reactors (Guckenheimer and Holmes, 1993). In our laboratory the critical flow rate is determined by a simple well-stirred glass reactor with 30 μl volume. An on-line measurement of the fluorescence intensity (using ToPro-1) allows *in situ* monitoring of the reaction while changing the flow rate. The 3SR was shown to amplify RNA and DNA products in a very stably manner (we observed the reaction for several hours) for appropriate flow rates. An increase in the flow rate does not disturb the reaction until a critical flow rate

is reached, then the concentrations of RNA and DNA are diluted by the outflux and the fluorescence intensity drops to zero.

Despite the fact that this it not the theme of this work we want to mention that the selection pressure among different species, which may occur by mutation are rather high in a flow reactor. Due to the continuously high RNA/DNA concentrations possible over long reaction time, a well-mixed flow reactor represents a valuable alternative to the serial transfer technique. In the next section we shall see that these considerations are especially important in the case of coupled systems in flow reactors.

3. COUPLED 3SR SYSTEMS

The design of a model system of coupled amplification cycles requires the functionality of the species involved to be linked directly to their ability to replicate. After execution of the function and running through the replication cycle, the species has to be returned to the initial state. The isothermal reaction scheme and flow conditions, as introduced at the end of Section 2, are necessary for this. The simplest way to design the coupling of two amplification systems according to a predator–prey model is to use a vital intermediate of one replication cycle as a primer for the second one. This means that the second replication cycle becomes the predator of the first one, the prey. In Fig. 3 this coupling method is presented. The prey cycle works as described above, see Fig. 1. All necessary compounds for the amplification, especially both primers, are provided. The predator cycle, on the other hand, is only provided with the primer for starting reverse transcription. The second primer is provided by the single-stranded template DNA_1 of the prey cycle. The sequence of this template DNA_1 is designed so that predator template DNA_2 and prey template DNA_1 are sharing a complementary sequence element at their 3′-ends. The consensus sequence of the promoter of the RNA-polymerase is located upstream of this complementary sequence element on DNA_1. After annealing DNA_2 and DNA_1, reverse transcriptase can synthesize the double-stranded substrate for RNA-polymerase, which can start the *in vitro* transcription of antisense predator-RNA.

The classic example of a predator–prey system is the well known Lotka–Volterra reaction system:

$$\begin{array}{lcl} X_1 & \xrightarrow{k_1} & 2X_1 \\ X_2 + X_1 & \xrightarrow{k_2} & 2X_2 \\ X_2 & \xrightarrow{\phi} & \emptyset. \end{array} \tag{25}$$

In the absence of the predator (X_2), the prey (X_1) grows exponentially. Conversely, the predator (X_2) can not grow without prey, but its growth rate increases proportionally to the prey. The system has two steady states; one saddle-point singularity at $x_2 = x_1 = 0$ and a second neutrally stable steady state at $x_2 = k_1/k_2$,

$x_1 = \phi/k_2$. The solution for initial values in the neighborhood of the neutrally stable steady state is an oscillatory behavior with period $T = 2\pi/\sqrt{k_1\phi}$ (Murray, 1993). In accordance with the flow terms discussed in Section 2, an outflow term for the prey may be added; the only effect is that we have to replace k_1 in the formulas above by $k_1 - \phi$.

While the Lotka–Volterra system (25) does not exhibit stable limit cycles, their existence is known to depend on more detailed models of the interaction and growth (Emlen, 1984). So we now turn to the detailed biochemical coupling, derived from the 'uncoupled' kinetics studied in Section 2:

$$
\begin{array}{lcll}
\mathrm{DNA}_1 & + \ \mathrm{P2} & \xrightarrow{k_1^a} & \mathrm{DNA}_1 : \mathrm{P2} \\
\mathrm{DNA}_1 : \mathrm{P2} & + \ \mathrm{RT} & \xrightarrow{k_2^a} & \mathrm{DNA}_1 : \mathrm{P2} : \mathrm{RT} \\
\mathrm{DNA}_1 : \mathrm{P2} : \mathrm{RT} & & \xrightarrow{k_3^a} & \mathrm{ds\,DNA}_1 + \mathrm{RT} \\
\mathrm{ds\,DNA}_1 & + \ \mathrm{T} & \xrightarrow{k_4^a} & \mathrm{ds\,DNA}_1 : \mathrm{T} \\
\mathrm{ds\,DNA}_1 : \mathrm{T} & & \xrightarrow{k_5^a} & \mathrm{RNA}_1 + \mathrm{T} + \mathrm{ds\,DNA}_1 \\
\mathrm{RNA}_1 & + \ \mathrm{P1} & \xrightarrow{k_6^a} & \mathrm{RNA}_1 : \mathrm{P1} \\
\mathrm{RNA}_1 : \mathrm{P1} & + \ \mathrm{RT} & \xrightarrow{k_7^a} & \mathrm{RNA}_1 : \mathrm{P1} : \mathrm{RT} \\
\mathrm{RNA}_1 : \mathrm{P1} : \mathrm{RT} & & \xrightarrow{k_8^a} & \mathrm{DNA}_1 + \mathrm{RT} \\
 & & & \\
\mathrm{DNA}_2 & + \ \mathrm{DNA}_1 & \xrightarrow{k_1^b} & \mathrm{DNA}_2 : \mathrm{DNA}_1 \\
\mathrm{DNA}_2 : \mathrm{DNA}_1 & + \ \mathrm{RT} & \xrightarrow{k_2^b} & \mathrm{DNA}_2 : \mathrm{DNA}_1 : \mathrm{RT} \\
\mathrm{DNA}_2 : \mathrm{DNA}_1 : \mathrm{RT} & & \xrightarrow{k_3^b} & \mathrm{ds\,DNA}_2 + \mathrm{RT} \\
\mathrm{ds\,DNA}_2 & + \ \mathrm{T} & \xrightarrow{k_4^b} & \mathrm{ds\,DNA}_2 : \mathrm{T} \\
\mathrm{ds\,DNA}_2 : \mathrm{T} & & \xrightarrow{k_5^b} & \mathrm{RNA}_2 + \mathrm{T} + \mathrm{ds\,DNA}_2 \\
\mathrm{RNA}_2 & + \ \mathrm{P3} & \xrightarrow{k_6^b} & \mathrm{RNA}_2 : \mathrm{P3} \\
\mathrm{RNA}_2 : \mathrm{P3} & + \ \mathrm{RT} & \xrightarrow{k_7^b} & \mathrm{RNA}_2 : \mathrm{P3} : \mathrm{RT} \\
\mathrm{RNA}_2 : \mathrm{P3} : \mathrm{RT} & & \xrightarrow{k_8^b} & \mathrm{DNA}_2\,.
\end{array}
\tag{26}
$$

The two 3SR replication cycles are as described above with a coupling of the Lotka–Volterra type given by the primer function of DNA_1. Without any flow terms the predator is strongly disadvantaged. The priming of the prey DNA (reaction rate k_1^a) and the priming of the predator DNA (reaction rate k_1^b) compete for the prey DNA. Both reactions are of second order, but the concentration of the primer P2 is several orders of magnitudes higher than the concentration of DNA_1 and DNA_2 (at least in the exponential growth phase for the prey). The part of prey DNA, which can be exploited by the predator is negligible. Thus, the predator can only grow, after the concentration of the primer P2 has dropped to

zero. This explains the fact that in batch experiments an effective predator/prey coupling can only be found in a narrow parameter range. The predator can grow only after the prey has stopped to grow, see Wlotzka and McCaskill (1997).

The situation changes in the case of a continuous operation in a well-stirred flow reactor. Appropriate flow conditions can fix the steady-state concentration of the prey cycle within a region which presents ideal conditions for the growth of the predator. Then the two amplification cycles should show an effective coupling of the Lotka–Volterra type. However, the situation is much more complicated than in the simple Lotka–Volterra system: further couplings are introduced by the common use of reverse transcriptase (RT) and RNA-polymerase (T); the exponential growth is limited by enzyme saturation and primer depletion. The dimension for the phase space of the full kinetic model is rather high and the trajectories in this phase space depend on the initial concentrations, the choice of the kinetic parameters and the flow conditions.

At first, it is not obvious that the above model will show any limit cycle oscillations. In contrast to the Lotka–Volterra model the prey can not grow infinitely, but is limited by the finite resource of the primer concentration. Resource-limited predator–prey systems have been studied in the context of population biology and do not cycle at all, see Emlen (1984) and literature therein. To see this for a biochemical system in a flow reactor let us study the small system

$$\begin{array}{lcll} X_1 & + \ \mathrm{R} & \xrightarrow{k_1} & 2\ X_1 \\ X_2 & + \ X_1 & \xrightarrow{k_2} & 2\ X_2 \\ X_1, X_2, \mathrm{R} & & \xrightarrow{\phi} & \emptyset \\ \emptyset & & \xrightarrow{\phi r_0} & \mathrm{R}, \end{array} \tag{27}$$

which has the same type of primer-limited prey growth and a Lotka–Volterra coupling as the full system (26). The non-trivial steady state of the system (27) is given by

$$x_1^* = \frac{\phi}{k_2}, \qquad x_1^* = \frac{k_1}{k_1 + k_2} r_0 - \frac{\phi}{k_2}, \qquad r^* = \frac{k_2}{k_1 + k_2} r_0. \tag{28}$$

There is a critical flow rate

$$\phi_c = \frac{k_1 k_2}{k_1 + k_2} r_0, \tag{29}$$

for which x_1^* drops to zero and the non-trivial steady state becomes identical to the trivial one. We non-dimensionalize by writing

$$\tau = \phi\, t, \qquad \tilde{x}_1 = x_1/r_0, \qquad \tilde{x}_2 = x_2/r_0, \qquad \tilde{r} = r/r_0 \tag{30}$$

and obtains the ODE

$$\begin{aligned}\frac{\partial\tilde{x}_1}{\partial\tau} &= \frac{k_1 r_0}{\phi}\,\tilde{x}_1\tilde{r} - \tilde{x}_1 - \frac{k_2 r_0}{\phi}\,\tilde{x}_1\tilde{x}_2\\ \frac{\partial\tilde{x}_2}{\partial\tau} &= \frac{k_2 r_0}{\phi}\,\tilde{x}_2\tilde{x}_1 - \tilde{x}_2\\ \frac{\partial\tilde{r}}{\partial\tau} &= -\frac{k_1 r_0}{\phi}\,\tilde{x}_1\tilde{r} + 1 - \tilde{r}.\end{aligned} \tag{31}$$

Let us now introduce two key parameters

$$\gamma = \frac{k_1}{k_2} \geq 0 \qquad \text{and} \qquad \delta = \frac{\phi_c}{\phi} = \frac{k_1 k_2 r_0}{(k_1 + k_2)\phi} \geq 1. \tag{32}$$

γ is a measure for the relative predator–prey coupling, whereas δ^{-1}gives the flux rate normed by the critical flow rate. Linearization about the non-trivial steady state yields the Jacobian

$$\mathbf{A} = \begin{pmatrix} 0 & -1 & \gamma \\ \delta - 1 & 0 & 0 \\ -\delta & 0 & -\gamma - 1 \end{pmatrix}. \tag{33}$$

The eigenvalues of $\mathbf{A}$

$$\lambda_1 = -1, \qquad \lambda_{2,3} = -\frac{\gamma}{2} \pm \frac{1}{2}\sqrt{(\gamma+2)^2 - 4\delta(\gamma+1)} \tag{34}$$

have only negative real parts and thus, system (27) can only exhibit damped oscillations. Note, that the imaginary parts of $\lambda_{2,3}$ are non-zero for

$$\delta \geq \frac{(\gamma+2)^2}{4(\gamma+1)}, \tag{35}$$

which corresponds to stable spiral trajectories near the steady state. Whereas the classical Lotka–Volterra model shows undamped oscillations, in the resource-limited predator–prey model (27) the oscillation is damped.

Table 1. Standard values of kinetic parameters used in the numerical simulations.

Parameter	Value
ϕ	$0.004\ \mathrm{s}^{-1}$ (flow rate)
$k_3^{a,b}$	$0.1\ \mathrm{s}^{-1}$
$k_5^{a,b}$	$0.02\ \mathrm{s}^{-1}$
$k_8^{a,b}$	$0.01\ \mathrm{s}^{-1}$
$k_i^{a,b}$ all higher-order reactions	$10^8\ \mathrm{mol}^{-1}\ \mathrm{s}^{-1}$

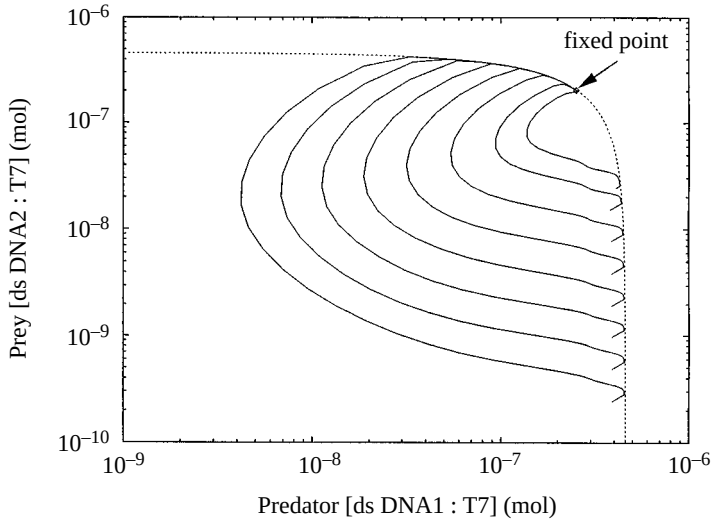

Figure 4. Predator–prey phase plane trajectories for the coupled 3SR reaction system. Plotted are the concentration of the complex $\mathrm{ds\,DNA_2 : T}$ (predator) versus the concentration of the complex $\mathrm{ds\,DNA_1 : T}$ (prey). The kinetic parameters are listed in Table 1 and the curve of concentrations, where the RNA-polymerase is saturated, given as a dotted line. Each of the eight trajectories start at a small prey concentration and end in the same steady state.

To gain an overall understanding of the coupled 3SR replication system we have performed numerical computations for the full reaction system (26) for numerous choices of the parameters. As an example, see Fig. 4 showing different phase plane trajectories of $[\mathrm{ds\,DNA_1 : T}]/[\mathrm{ds\,DNA_2 : T}]$. Here we chose a set of realistic kinetic parameters listed in Table 1. The initial primer and enzyme concentrations are chosen according to (14) for $K_1 = 10.66$ and $K_2 = 10.99$. None of the species are assumed to be immobilized and only the enzymes and the primers are included in the inlet flow. The curves in Fig. 4 each start at a rather high concentration of the predator, but a different prey concentration. The form of these trajectories are very similar: first the concentration of $\mathrm{ds\,DNA_2 : T}$ (predator) reaches the RNA-polymerase saturation curve, given by $[\mathrm{ds\,DNA_1 : T}] + [\mathrm{ds\,DNA_2 : T}] = [\mathrm{T}]_0$ and plotted as a dotted line. Then the predator concentration decreases due to the flux term and lack of prey. As the predator concentration drops the prey concentration starts to increase causing the predator to rise again and the phase plane trajectories reach the RNA-polymerase saturation curve for $[\mathrm{ds\,DNA_1 : T}] > [\mathrm{ds\,DNA_2 : T}]$. Here the concentration of $\mathrm{ds\,DNA_1 : T}$ can not grow any longer and the trajectories go along the RNA-polymerase saturation curve into a stable steady state.

The form of the trajectories change when we increase k_1^b to 3×10^8 mol^{-1} s^{-1}, see Fig. 5. In this case, the steady states do not lie on the RNA-polymerase saturation curve and the trajectories spiral into the steady state. Increasing further k_1^b to 6×10^8 mol^{-1} s^{-1} yields stable limit cycle oscillations, see Fig. 6. The

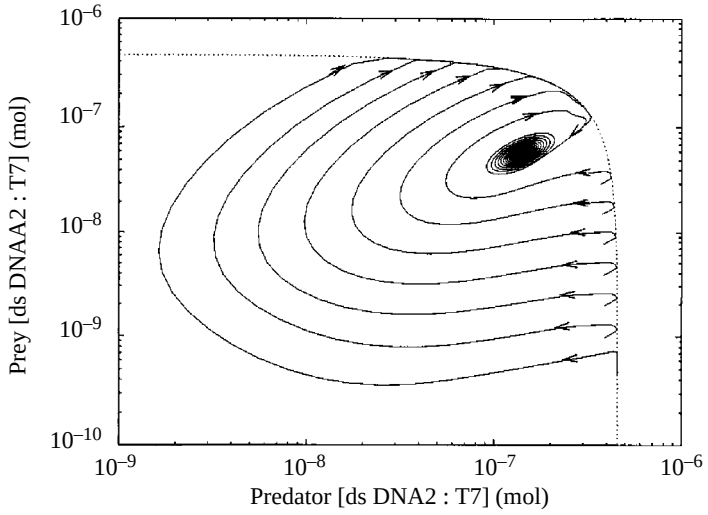

Figure 5. The same plot as in Fig. 3, but with $k_1^b = 3 \times 10^8$ mol^{-1} s^{-1}. Thus, the efficiency of the predator to catch prey is increased by a factor of 3. Here the trajectories turn in stable spirals to the fixed point.

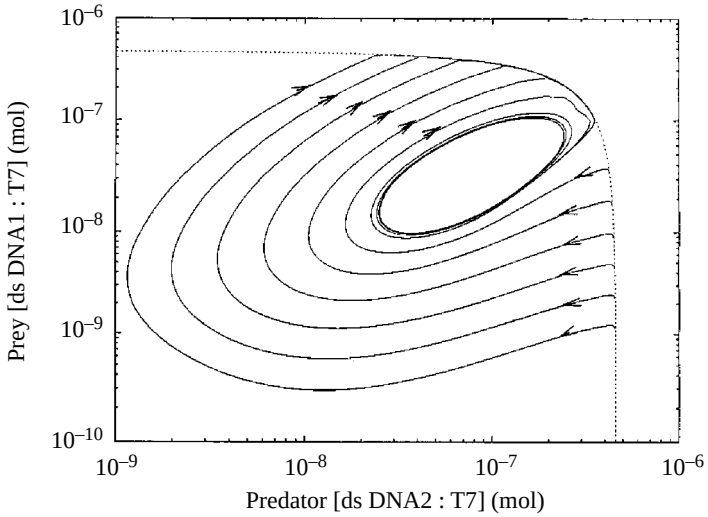

Figure 6. The same plot as in Figs 3 and 4, but with $k_1^b = 6 \times 10^8$ mol^{-1}s^{-1}. Now the trajectories show oscillatory behavior, see text.

oscillation only occurs for sufficient large flow rates. This is easy to understand, since the RNA production rate of prey and predator become rather independent if the death rates of the double-stranded DNAs of both cycles are too small. Adding inverse reactions to each association reaction does not destroy the oscillation. Surprisingly the fixed point becomes stable when the predator's ability to catch and convert the prey is increased, for example the choice $k_i^b = \alpha k_i^a, \quad i = 1, 2, \ldots, 8$ with a sufficient large factor α dampens the oscillation. The qualitative behavior of the phase-plane trajectories shown in Figs 4 and 5 are found in the small predator–prey model (27), whereas the limit cycle oscillation shown in Fig. 6, on the other hand, only occur in the full system. What is the mechanism producing the limit cycle oscillation shown in Fig. 6?

One possibility is that the coupling arises from the use of identical enzymes (RNA-polymerase and reverse transcriptase) in the predator and prey replication schemes; one cycle may act as an inhibitor for the other one thus producing an additional coupling. Experimentally this could be examined by applying distinct enzymes in the prey and predator 3SR cycles. By simulating the corresponding reaction system we observed no effect on the limit cycle oscillation. The only remaining explanation for the differences in the qualitative kinetic of the small model (27) and the full model (26) is the difference in the functional predator response. In the small system (27), the predator production rate depends linearly on the prey concentration throughout its range. In the full system (26) this is not longer valid. For small predator and large prey concentrations, the fast complex binding reactions result in a saturation of the predator. This leads to a kind of Michaelis–Menten substrate saturation for a small predator concentration, where the predator production rate depends only on the predator concentration itself but not on the prey concentration. This kind of coupling can be modeled by the small reaction system

$$\begin{array}{llllll} X_1 & + & \mathrm{R} & \xrightarrow{k_1} & Y_1 \xrightarrow{k_3} & 2X_1 \\ X_2 & + & X_1 & \xrightarrow{k_2} & Y_2 \xrightarrow{k_4} & 2X_2 \\ X_i, Y_i, \mathrm{R} & & & \xrightarrow{\phi} & \emptyset & i = 1, 2 \\ \emptyset & & & \xrightarrow{\phi\, r_0} & \mathrm{R}\,. & \end{array} \tag{36}$$

As numerical simulations show, this reaction system can oscillate. Let us study the system in some detail. The steady state of interest is given by

$$r^* = \frac{k_2(k_4 - \phi)r_0}{k_1(k_4 + \phi) + k_2(k_4 - \phi)}, \qquad x_1^* = \frac{\phi(k_4 + \phi)}{k_2(k_4 - \phi)}, \qquad y_1^* = \frac{k_1}{k_3 + \phi} x_1^* r^*, \tag{37}$$

$$x_2^* = \frac{k_1(k_3 - \phi)}{k_2(k_3 + \phi)} r^* - \frac{\phi}{k_2}, \; y_2^* = \frac{k_2}{k_4 + \phi} x_1^* x_2^*. \tag{38}$$

Linearization about the steady state yields the Jacobian

$$\mathbf{A} = \begin{pmatrix} -k_1 r^* - k_2 x_2^* - \phi & -k_2 x_1^* & 2k_3 & 0 & -k_1 x_1^* \\ -k_2 x_2^* & -k_2 x_1^* - \phi & 0 & 2k_4 & 0 \\ k_1 r^* & 0 & -k_3 - \phi & 0 & k_1 x_1^* \\ k_2 x_2^* & k_2 x_1^* & 0 & -k_4 - \phi & 0 \\ -k_1 r^* & 0 & 0 & 0 & -k_1 x_1^* - \phi \end{pmatrix}. \tag{39}$$

The matrix $\mathbf{A}$ depends parametrically on k_1, k_2, k_3, k_4, r_0 and ϕ; two of them can be eliminated by non-dimensionalizing the problem. We reduce the number of parameters by fixing the flow rate and the parameters of the prey

$$r_0 = 10^{-6}\ \text{mol}, \qquad k_1 = 10^8\ \text{mol}^{-1}\ \text{s}^{-1}, \qquad k_3 = 0.01\ \text{s}^{-1}, \qquad \phi = 0.005\ \text{s}^{-1} \tag{40}$$

to values similar to those used in the full system (see Table 1) and vary the two parameters

$$\gamma = k_2/k_1, \qquad \rho = k_4/k_3. \tag{41}$$

In particular, we are we looking for parameters γ and ρ for which the steady state becomes unstable, for example for which at least one of the eigenvalues of the Jacobian $\mathbf{A}$ has a positive real part. The behavior of the system when γ and ρ vary is shown in the bifurcation diagram plotted in Fig. 7. The two-dimensional phase space is segmented into three domains. For $\rho \leq 0.5$ the efficiency of the predator in converting food (prey) becomes too low and the predator dies due to the outflow. For small γ or large ρ the fixed point is stable but in the case of increased γ it can become unstable through a saddle-point bifurcation (solid line). It turns out that for each fixed parameter ρ in the range $0.5 \leq \rho \leq 2.5$ the Jacobian has at least one eigenvalue pair with a positive real part for γ which is sufficiently large ($\gamma > \gamma_{\text{thr}}(\rho)$). The threshold function $\gamma_{\text{thr}}(\rho)$ (given by the line of the saddle-point bifurcation) determines the minimal relative predator–prey coupling γ for which oscillation can be expected. Note that according to Fig. 7, stability is more likely to occur for larger ρ values. This observation is in agreement with the behavior of the full system which was found in the numerical simulation, but, on the other hand, runs in contrast to the results of conventional predator–prey models (Emlen, 1984): system (36) is more apt to be stable if the predator *is* highly efficient in converting food (prey) to growth and reproduction.

Of special experimental interest is the dependency of the system on the flow rate, which can be easily varied in a flow reactor. Thus, let us fix the ratio $\rho = k_4/k_3$ to one ($k_4 = k_3$) and vary the flow rate. The corresponding bifurcation diagram is shown in Fig. 8. Obviously the concentrations drop to zero beyond the critical flow rate $\phi \approx 0.01$ (broken line). Below the critical flow rate the fixed point is stable for small values of γ. By increasing γ the fixed point becomes unstable when the saddle-point bifurcation (solid line) is crossed. Note, that the flow rate determines the frequency of the oscillation and for the observation of

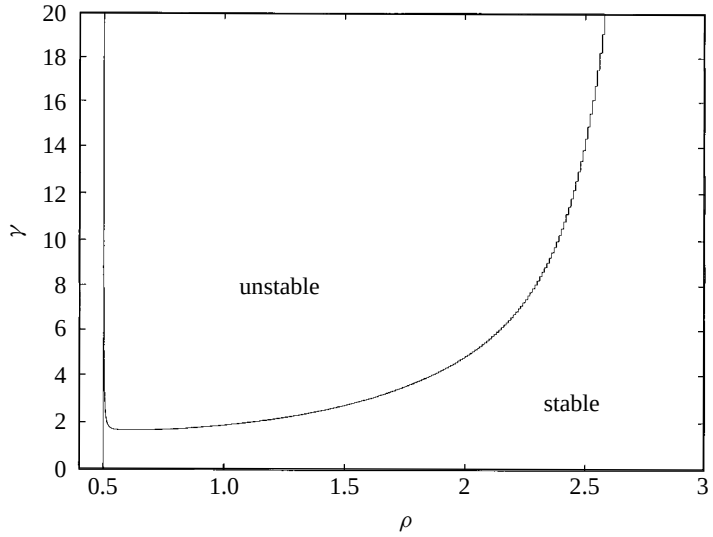

Figure 7. The region of stability and instability of the steady state (37) of the small reaction system (36) in the γ–ρ plane. The parameter $\gamma = k_2/k_1$ gives the relative efficiency of the predator to catch the prey, whereas $\rho = k_4/k_3$ gives the relative efficiency of the predator at converting food (prey) for growth and reproduction. The two-dimensional phase space is segmented into three domains. For $\rho \leq 0.5$ the efficiency of the predator in converting food (prey) becomes too low and the predator dies due to the outflow. For small γ or large ρ the fixed point is stable but in the case of increased γ it can become unstable through a saddle-point bifurcation (solid line). Note, that the system is more apt to be stable for large ρ values.

such oscillations it is advantageous to choose the flow rate as large as possible. Figure 8 shows that the unstable region can be reached with $\gamma < 2.0$ nearly up to the critical flow rate.

4. Discussion and Conclusion

This work is based on the analysis of a kinetic model for the experimental 3SR reaction. However the detailed comparison of this model with experimental data is not the focus of the current work. That the model captures the essentials of isothermal amplification in the 3SR reaction can be verified by the reader by comparing with Guatelli *et al*. (1990); Ehricht *et al*. (1997); Gebinoga and Oehlenschläger (1996). Based on the kinetic model, a coupled *in vitro* DNA-based predator–prey system has been studied. An experimental paper is in preparation where both the detailed kinetics of the 3SR reaction and the predator–prey coupled system have been investigated by detailed radio-labeled tracing (Wlotzka and McCaskill, 1997). The model system has been realized experimentally as described in Fig. 3. Under batch and flow conditions, evidence for the coupling of both cycles could be found. Further work involving a search for optimal con-

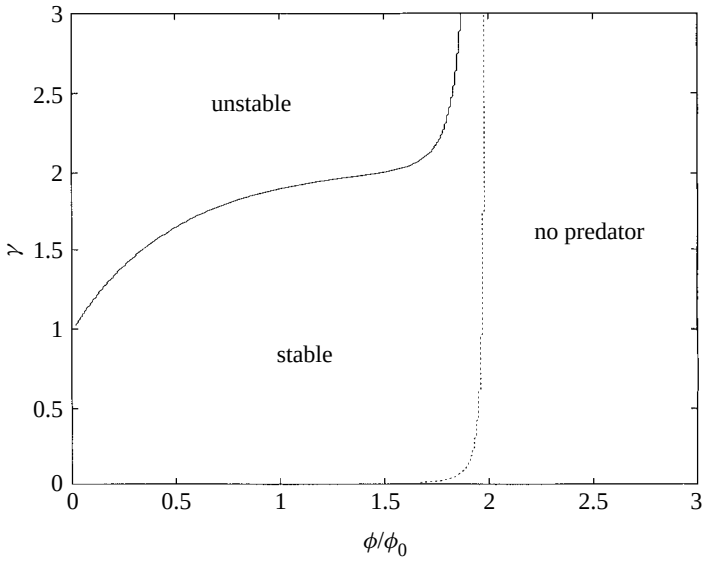

Figure 8. The region of stability and instability of the steady state (37) of the small reaction system (36) in the γ–ϕ plane. The parameter $\gamma = k_2/k_1$ gives the relative efficiency of the predator to catch the prey, whereas ϕ is the flow rate measured in units of $\phi_0 = 0.005\ \mathrm{s}^{-1}$. The concentrations drop to zero beyond the critical flow rate $\phi \approx 0.01$ (broken line). Below the critical flow rate the fixed point is stable for small values of γ. By increasing γ the fixed point becomes unstable when the saddle-point bifurcation (solid line) is crossed. The unstable region can be reached with $\gamma < 2.0$ nearly up to the critical flow rate.

ditions for stable oscillation will be based on the theoretical analysis presented in the current contribution. The current work is therefore not based on hypothetical reaction schemes, but represents a theoretical contribution predicting oscillatory behavior in an experimental system under current investigation.

The choice of mass-action kinetics described using ODEs is conventional, but the reader should consult reference Wu and Kapral (1994) for example, for a discussion of possible complications. We have ignored stochastic effects in the above analysis, which will certainly become important in extensions of the model to evolutionary questions, see below. Much modeling of predator–prey systems in the biological literature is in terms of delay equations, which are not usual in chemical kinetics. The relationships to the treatment in terms of continuous differential equations, however, are well documented in the literature (Murray, 1993).

Numerical simulation of the full kinetic model shows stable oscillatory kinetics (a limit cycle). In general, limit cycle kinetics of predator–prey-like systems show significant dependence on the details of the model used and so it was important to describe a multicomponent model with realistic kinetics to establish this behavior for a real evolutionary biochemical system. Hypercycle models, for example, require more than four coupled species for oscillations to occur Eigen

and Schuster (1977, 1978a; 1978b). The mechanism of the oscillation has been analyzed and can be described by a simple model. The critical kinetic parameter for the oscillation is the efficiency of the predator to catch prey, whereas a high efficiency of the predator to convert the prey stabilizes the non-oscillatory state of the system. There exists a minimum flow rate for oscillatory kinetics, so that the embedding of the biochemistry in a flow reactor is essential. Above a certain critical flow rate, as described in Section 2, all species are diluted out, so that the results predict a range of flow rates to be used as a guide in optimizing experimental systems. Further simulations have shown that the results are comparatively insensitive with the reversal of the bimolecular association steps (primer annealing and enzyme binding) even when these reverse dissociation reactions proceed faster than the polymerizations processes. Choice of primer sequences and enzyme concentrations can significantly bias the rates of reactions, so that the optimization criteria derived in this work can be used practically to guide decisions in the construction of oscillatory kinetics.

Biochemical oscillations have been studied in great detail since the early work on glycolysis (Goldbeter, 1996). The oscillatory mechanism proposed in this work is of the quadratic rather than cubic catalysis type (Gray and Scott, 1985). Chemical chaos (Swinney, 1984; Olsen, 1983) is unlikely in the system investigated here, and did not show up in the numerical simulations. The significance of this work revolves around the fact that a realistic model of an evolvable biochemical system has been shown to undergo stable limit cycle oscillations. In an evolutionary context, oscillations have a major impact on the selection process. The existence of limit cycle oscillations in the kinetics can also lead to spatial pattern formation processes which give rise to totally new phenomena at the level of molecular selection. In cooperative systems, for example, it has been shown that functional cooperation between molecules can be stabilized by this means (Boerlijst and Hogeweg, 1991; Böddeker and McCaskill, 1998). Evolution experiments on laboratory timescales have been made possible by the discovery of simple isothermal amplification schemes such as the 3SR reaction, so that the tenants of evolutionary population ecology will be testable in the near future in chemical terms.

In this work we summarize the considerations, which have been helpful for the recent construction and optimization of the coupled isothermal amplification of nucleic acids in our laboratory (Wlotzka and McCaskill, 1997), see also Ehricht *et al*. (1997); Wright and Joyce (1997); Ellington *et al*. (1997) and references therein. Starting with the knowledge of the dynamic behavior of the components of a single 3SR a coupling to a predator has been selected. The weakness of the competitive predator/prey coupling in batch experiments is well understood by our model and leads to the realization, that a flow reactor is essential for an effective molecular predator/prey system. The most critical parameter for the asymptotic behavior of the system is the efficiency of the predator to catch the prey. In the case of small efficiency [given by a small parameter γ in the

small system (36)] both predator and prey have a stable non-zero concentration for $t \to \infty$. When the efficiency γ is increased the fixed point becomes unstable and the concentrations oscillate. The velocity of annealing predator and prey depends strongly on the matching sequences. Thus, the parameter γ can be influenced by choosing corresponding sequences for the biochemical predator/prey system. Note also, that the molecular evolution of the predator will lead to a higher efficiency of the predator to catch the prey and, thus, will lead to an increasing value of γ. Reaching the unstable region, the oscillations and the possible pattern formations in a spatial (two-dimensional/three-dimensional) flow reactor may result in a complex evolution of the kinetic, the sequences and the spatial structure of the system.

First flow experiments have been performed with a single as well as with the coupled system. In both cases the amplification turns out to be very stable and a critical flow rate can be measured. For appropriate flow conditions the concentration of the prey as well as the concentration of the predator can both be kept simultaneously on a rather high value, which is a promising result in view of a future detection of oscillation or pattern formation for this system. At present our group is studying the evolutionary stability of the coupled system and planning experiments for the detection of oscillation. To minimize the cost of such experiments micro-structured flow reactors with immobilized enzymes are currently designed and produced in our laboratory, see also Foerster *et al*. (1994).

ACKNOWLEDGEMENTS

JA was supported by a grant from the German Bundesministerium für Bildung und Forschung, and gratefully acknowledges their assistance.

REFERENCES

Biebricher, Ch. K., M. Eigen and W. C. Gardiner Jr (1983). Kinetics of RNA replication. *Biochemistry* **22**, 2544.

Biebricher, Ch. K., M. Eigen and W. C. Gardiner Jr (1984). Kinetics of RNA replication: plus–minus asymmetry and double-stranded formation. *Biochemistry* **23**, 3186.

Biebricher, Ch. K., M. Eigen and W. C. Gardiner Jr (1985). Kinetics of RNA replication: competition and selection among self-replication of RNA species. *Biochemistry* **24**, 6550.

Böddeker, B. and J. S. McCaskill (1998). Do self–replicant spots provide a plattform for heriditary molecular diversity? *J. Theor. Biol.*, in press.

Boerlijst, M. C. and P. Hogeweg (1991). Spiral wave structure in pre–biotic evolution: hypercycles stable against parasites. *Physica* **D48**, 17.

Bray, W. C. (1980). Hypercycles, parasites and packages. *J. Theor. Biol.* **85**, 399.

Ehricht, R., Th. Ellinger and J. S. McCaskill (1997). Cooperative amplification of templates by cross-hybridization (CATCH). *Eur. J. Biochem.* **243**, 358.

Eigen, M. (1989). The molecular quasispecies. *Adv. Chem. Phys.* **75**, 149.

Eigen, M. (1971). The quasispecies model. *Naturwissenschaften* **58**, 465.

Eigen, M. and P. Schuster (1977). The hypercycle: A principle of natural self–organisation. *Naturwissenschaften* **64**, 541.

Eigen, M. and P. Schuster (1978a). *Naturwissenschaften* **64**, 7.

Eigen, M. and P. Schuster (1978b). *Naturwissenschaften* **65**, 341.

Ellington, A. D., M. P. Robertson and J. Bull (1997). Ribozymes in wonderland. *Science* **276**, 546.

Emlen, J. M. (1984). *Population Biology*. MacMillan, New York, USA.

Foerster, P., B. Wlotzka and J. S. McCaskill (1994). Spatially resolved evolution studies in an open reactor. *Ber. Bunsenges. Phys. Chem.* **98**, 1203.

Gebinoga, M. and F. Oehlenschläger (1996). Comparisons of 3SR reaction systems. *Eur. J. Biochem.* **235** , 256.

Goldbeter, A. (1996). *Biochemical Oscillations and Cellular Rhythms. The Molecular Bases of Periodic and Chaotic Behaviour*. New York: Cambridge University Press.

Gray, P. and S. K. Scott (1985). Sustained oscillations and other exotic patterns of behavior in isothermal reactions. *J. Chem. Phys.* **89**, 22.

Guatelli, J. C., K. M. Whitefield, D. Y. Kwoh, K. J. Barringer, D. D. Richman and T. R. Gingeras (1990). Isothermal, *in vitro* amplification of nuclei acids by a multienzyme reaction modeled after retroviral replication. *Proc. Natl. Acad. Sci. USA* **87**, 1874.

Guckenheimer, J. and P. Holmes (1993). *Nonlinear Oscillations, Dynamical Systems, and Bifurcation oc Vector Fields*, volume 42 of *Applied Mathematical Science*, New York: Springer.

Hofbauer, J. and K. Sigmund (1988). *The Theory of Evolution and Dynamical Systems*, Cambridge: University of Illinois Press.

Lotka, A. J. (1910). Contribution to the theory of periodic reactions. *J. Phys. Chem.* **14**, 271.

Lotka, A. J. (1920). Undamped oscillation derived from the law of mass action. *J. Amer. Chem. Soc.* **42**, 201.

Luisi, P. L., P. Walde and T. Oberholzer (1994). Enzymatic RNA synthesis in self–reproducing vesicles: an approach to the construction of a minimal synthetic cell. *Ber. Bunsenges. Phys. Chem.* **98**, 1160.

Murray, J. M. (1982). Parameter space for Turing instability in reaction-diffusion mechanisms: a comparison of models. *J. Theor. Biol.* **98**, 1431.

Murray, J. M. (1993). 2nd edn. *Mathematical Biology*, Berlin: Springer.

Olsen, L. F. (1983). An enzyme reation with strange attractor. *Phys. Lett.* **94**, 454.

Spiegelmann, S. (1971). An approach to the experimental analysis of precellular evolution. *Q. Rev. Biophys.* **4**, 213.

Swinney, H. S. (1984). Chemical chaos, in *Non-equilibrium Dynamics in Chemical Systems*, C. Vidal and A. Pacault (Eds), p. 124. Berlin: Springer.

Volterra, V. (1926). Variazionie fluttuazioni del numero d'individui in specie animali conviventi. *Mem. Acad. Lincei.* **2**, 31.

Volterra, V. (1931). Variations and fluctuations of a number of individuals in animal species living together, in *Animal Ecology*, R. N. Chapman (ed.), New York: McGraw Hill, p. 409.

Wlotzka, B. and J. S. McCaskill (1997). A molecular predator and its prey: coupled isothermal amplification of nucleic acids. *Biology & Chemistry* **4**, 25.

Wright, M. C. and G. F. Joyce (1997). Continuous in vitro evolution of catalytic function. *Science* **276**, 614.

Wu, X. G. and R. Kapral (1994). Effects of molecular fluctuations on chemical oscillations and chaos. *J. Chem. Phys.* **100**, 5936.

Received 28 July 1996 and accepted 12 October 1997